Improving Auditory Steady-State Response Detection Using Independent Component Analysis on Multichannel EEG Data

Bram Van Dun*, *Student Member, IEEE*, Jan Wouters, and Marc Moonen, *Senior Member, IEEE*

***Abstract*—Over the last decade, the detection of auditory steady-state responses (ASSR) has been developed for reliable hearing threshold estimation at audiometric frequencies. Unfortunately, the duration of ASSR measurement can be long, which is unpractical for wide scale clinical application. In this paper, we propose independent component analysis (ICA) as a tool to improve the ASSR detection in recorded single-channel as well as multichannel electroencephalogram (EEG) data. We conclude that ICA is able to reduce measurement duration significantly. For a multichannel implementation, near-optimal performance is obtained with five-channel recordings.**

***Index Terms*—Auditory steady-state response, electroencephalogram, independent component analysis, multichannel.**

I. Introduction

In 1994 the Joint Committee on Infant Hearing (JCIH) stated that universal detection of infants with hearing loss is recommended before the age of three months [1]. However, universal newborn hearing screening programs are only efficient if an appropriate intervention can follow after an accurate diagnosis is made. Based on this assessment, e.g., an effective fitting of a hearing aid can be carried out, which is an otherwise difficult task with very young children. Nowadays, the most important diagnostical techniques to assess hearing in young infants include otoacoustic emissions (OAE), the (click-evoked) auditory brainstem response (ABR), and the auditory steady-state response (ASSR). These methods are to some extent complementary to each other. Distortion product OAE (DPOAE) are, in contrast with transient evoked OAE (TEOAE), frequency-specific. Unfortunately, this frequency-specificity is not correlated with the hearing threshold of the observed subject and not observable at hearing losses from 40 dBHL and higher. While the nonfrequency-specific ABR is generally used for screening purposes and a more general assessment of hearing thresholds, the frequency-specific ASSR makes a fairly accurate guess of hearing thresholds at different frequencies in an acceptable time (i.e., less than 1 hr.) [2], [3].

ASSRs are faint evoked electrical responses of the brain to auditory stimuli "whose constituent discrete frequency components remain constant in amplitude and phase over an infinitely long time period" [4]. Their magnitude is in the order of nanovolts. For practical purposes, a response is considered stable when measured over a duration considerably longer than a single stimulus cycle. These responses can be elicited by amplitude and/or frequency modulated (AM, FM) pure tones. If a tested carrier frequency is modulated with a lower modulation frequency, the appearance of this modulation frequency in the monitored EEG is a strong indication that the subject has effectively perceived the carrier. Several studies have shown that modulation frequencies above 80 Hz lend themselves well to audiometry, especially with young children [5]–[10]. Unfortunately, the measurement time for a single-stimulus technique is unacceptably long, as at least four frequencies need to be administered to each ear to obtain appropriate audiogram information.

A solution to this problem is to record the responses to different carrier frequencies in both ears simultaneously by modulating each signal with a different modulation frequency [11], [12]. This technique reduces the test duration by a factor of two or three [13]. When different statistical methods and averaging techniques are considered, the best results are obtained when noise weighted averaging is used together with a statistical test that takes both signal phase and magnitude into account (like the F-test or magnitude square coherence) [14]–[17]. However, these improvements are rather marginal.

Different stimulus waveforms can elicit larger responses. Response amplitude increases of 30% using exponential modulation envelopes or signal-to-noise ratio (SNR) improvements up to 60% using multiple AM carriers are possible [18]–[20]. If the intensities of the stimuli are manipulated individually within a maximum mutual range of 20 dB, a shorter measurement session is possible. With this manipulation, the measurement protocol has the possibility to stop collecting data for a certain carrier frequency when its response is already significant. This can occur before the predefined amount of data for the current intensity is collected or before all other responses to their corresponding frequencies have become significant. The intensity of the specific carrier frequency is immediately reduced as soon as a response is detected [13], [21].

The most common electrode position for ASSR measurements is the Cz-inion position with Pz as ground electrode. However, the question arises if other electrode combinations

Manuscript received February 24, 2006; revised October 22, 2006. This work was supported in part by the Institute for the Promotion of Innovation through Science and Technology in Flanders (IWT-Vlaanderen); in part by the FWO under Grant G.0504.04 (design and analysis of signal processing procedures for objective audiometry in newborns); and in part by the Concerted Research Action GOA-AMBioRICS. *Asterisk indicates corresponding author.*

*B. Van Dun is with Experimental ORL (ExpORL) of the Neurosciences Department, and SCD-SISTA of the Electrical Engineering Department (ESAT), Katholieke Universiteit Leuven, 3000 Leuven (e-mail: bram.vandun@med.kuleuven.be).

J. Wouters is with Experimental ORL (ExpORL) of the Neurosciences Department, Katholieke Universiteit Leuven, 3000 Leuven, Belgium.

M. Moonen is with SCD-SISTA of the Electrical Engineering Department (ESAT), Katholieke Universiteit Leuven, 3001 Leuven, Belgium.

Digital Object Identifier 10.1109/TBME.2007.897327

0018-9294/$25.00 © 2007 IEEE

TABLE I
RECORDING ELECTRODE POSITIONS FOR A SEVEN-CHANNEL SETUP. ALL CHANNELS ARE REFERENCED TO THE COMMON ELECTRODE ON THE FOREHEAD. THE CONFIGURATION FOR THE SINGLE-CHANNEL SETUP IS DENOTED USING BOLD TYPEFACE

channel	position
1	**Oz**
2	P4
3	P3
4	**Cz**
5	F4
6	F3
7	Pz
common	**forehead**
ground	left mastoid

may actually yield a higher SNR and, thus, a faster detection of the response. According to [22], the highest SNR for infants younger than six months are recorded from the mastoids ipsilateral to the ear of stimulation referenced to Cz. For adults, the common positions are valid [23].

When adaptive regularized least-squares filtering is used, simulations with EEG data show that a significant improvement is possible [24].

Over the last decade, independent component analysis (ICA) [25] has appeared as a powerful signal analysis tool for a variety of industrial, medical and even financial applications, e.g., [26]–[29]. ICA allows finding the underlying factors from multivariate statistical data by looking for components that are both statistically independent, and non-Gaussian. In the present study, the possible use of ICA in ASSR detection is investigated. First, the available seven-channel data of 8 normal-hearing subjects are processed based on ICA (using the JADE algorithm) and results are compared to those from the most common single-channel ASSR technique [30]. It will be shown that ICA significantly improves detection for measurements between 30 and 60 dBSPL. Second, the optimal number of input channels, the optimal electrode positions and the optimal number of independent components are reported. Third, by fixing the separating matrix $\mathbf{W}$, calculated from data with a high SNR, a performance improvement may be expected. This assumption is evaluated. Fourth, the performance of an ICA-based procedure applied to single-channel data is considered. Finally, a combination of previous techniques is presented.

II. METHODS

A. Experimental Setup

The ASSR measurements were conducted in a sound-proof Faraday cage. The recording-electrode placement can be found in Table I, in accordance with the international 10-20 system [31]. All seven active electrodes were referenced to the common electrode, which was placed on the forehead. The Kendall electrodes were placed on the subject's skull after the skin was abraded with Nuprep abrasive skin prepping gel. A conductive paste was used to keep the electrodes in place and to avoid that inter-electrode impedances exceeded 5 $\mathrm{k}\Omega$ at 30 Hz. The electrodes were connected to a low-noise Jaeger-Toennies multichannel amplifier. Each EEG channel was amplified ($\times$ 10 000), bandpass filtered between 70 and 120 Hz (6 dB/octave) and finally software highpass filtered at 75 Hz (60 dB/octave). The amplified EEG signals were read using an RME Hammerfall DSP Multiface multichannel sound card and recorded using Adobe Audition 1.0 at a sampling rate of 32 kHz and downsampled to 250 Hz. Downsampling does not influence the performance of the ICA algorithm, but greatly improves its efficiency. All offline processing was performed using Matlab R14. The sound card was also used to generate the stimuli (see below). An artefact rejection protocol was used. All epochs, data blocks of 256 samples, greater than 20 μV in absolute value were rejected. The acquired signals were divided in sweeps of 16.384 s and averaged. A fast Fourier transform (FFT) analysis was carried out and a response was considered present if the F-ratio statistic (F-test with 2 and $2N-1$ degrees of freedom) showed a significant difference between the response power and the mean noise power of $N = 120$ neighboring frequency bins, approximately 3.7 Hz (60 bins) at each side [30]

$$F_{\mathrm{ratio}} = \frac{a^2_{\mathrm{response}}}{\frac{1}{N}\sum_{i=1}^{N} a^2_{\mathrm{noise}_i}} \tag{1}$$

with a_{response} the amplitude of the response being tested and a_{noise_i} the amplitude noise at each of the i adjacent frequency bins.

Eight normal-hearing volunteers (age range 22-33 years) participated in the study. Their behavioral hearing thresholds were less than 20 dBSPL for octave audiometric frequencies between 500 and 4000 Hz. Subjects were asked to lie down on a bed with eyes closed and to relax or sleep. Four trials with a length of 48 sweeps each (approximately 13 min) were conducted: at 60, 50, 40, and 30 dBSPL respectively. These intensities were chosen as the main goal of the study was to decrease the measurement duration, and not hearing threshold assessment in general. At the end of the session, behavioral thresholds were determined at 0.5, 1, 2, and 4 kHz with a 5 up-10 down method using modulated sinusoids.

B. Stimuli

Two stimuli with four 100% amplitude modulated (AM) carrier frequencies each, were applied to each ear. The carrier frequencies were the same for both ears; namely, 0.5, 1, 2, and 4 kHz. The modulation frequencies were taken close to respectively 82, 90, 98 and 106 Hz for the left ear, and 86, 94, 102 and 110 Hz for the right ear. To obtain an integer number of modulation frequency cycles in one data block of 256 samples (1.024 s), the previous values had to be corrected slightly [30]. This stimulus configuration was used with four out of eight subjects. The other four subjects received a reduced stimulus set, with only 0.5 and 4 kHz applied to the left ear and 1 and 2 kHz to the right ear. This difference in stimulus sets does not influence the following results.

Stimuli were created using Matlab R14 and played using Adobe Audition 1.0 at a sampling rate of 32 kHz. An RME Hammerfall DSP Multiface multichannel sound card sent the stimuli to Etymotic Research ER-3A insert phones for subject stimulation. The eight separate signals were calibrated at 70 dBSPL, using a Brüel and Kjær Sound Level Meter 2260 in combination with a 2-cc coupler DB138.

C. Independent Component Analysis

1) Theory: ICA is a blind source separation technique that is used to find a latent structure underneath a set of observations [25], [32]. This underlying structure comes in the form of unknown sources or independent components (ICs). The ICA general model is

$$\mathbf{x} = \mathbf{f}(\theta, \mathbf{s})$$

with $\mathbf{x}^T = [x_1\ x_2, \ldots, x_n]$ a vector of n observations x_i and $\mathbf{f}$ an unknown function with parameters θ that operates on statistically independent underlying variables $\mathbf{s}^T = [s_1\ s_2, \ldots, s_m]$ with $m \leq n$. If $\mathbf{f}$ is a linear function, a special case of the above equation is obtained; namely

$$\mathbf{x} = \mathbf{A}\mathbf{s} \tag{2}$$

with $\mathbf{A}$ an $n \times m$ mixing matrix. The pseudoinverse $\mathbf{W} = \mathbf{A}^+$ is defined as the separating matrix. This formula states that each of the observations x_i is a linear combination of a set of m underlying ICs s_j

$$x_i = a_{i1}s_1 + \cdots + a_{im}s_m \quad \text{for} \quad i = 1, \ldots, n.$$

ICA algorithms estimate both $\mathbf{s}$ and $\mathbf{A}$.

The most important assumption of ICA is that the components, lineary combining into observations, are mutually independent of each other. The fundamental problem is how to assess the independence of the components. The more common approach assumes the distributions of the ICs to be as far from normal Gaussian as possible. This idea is fed by the inverse of the central limit theorem, which states that the distribution of a sum of independent variables shifts to a normal (Gaussian) distribution when the number of variables goes to infinity [33]. To make this approach practically usable, different approximate measures of non-Gaussianity have been developed. By maximising such a measure, a vector $\mathbf{s}$ can be constructed numerically. The ICA algorithm that has been used in the rest of this study is the joint approximate diagonalisation of eigenmatrices (JADE) algorithm [34]. This algorithm has advantages over, e.g., FastICA [35] that practically suffers much more from local optima, leading to the calculation of different ICs and separating matrices $\mathbf{W}$ when the algorithm is run several times over the same dataset. However, alternative algorithms could have returned a higher performance than JADE, like the recent MILCA algorithm [36]. It is possible to tailor the ICA algorithm to specific needs of the problem using the Bayes theorem [37]. An extension of ICA to underdetermined mixtures is also a possible approach [38], [39]. At the time of this research, JADE was considered a proven technique that was tested on several applications, while the new methods above did not have those benefits that much.

2) Multichannel ICA: The n-channel recordings are divided in sweeps and each sweep is averaged with all preceding sweeps from the same channel (Section II-A). The JADE algorithm takes such an averaged n-channel sweep as its input. Then m ICs are calculated. A separate F-test is conducted on each modulation frequency from each IC using its F-ratio (1) and calculating its F-value. For each modulation frequency, the largest F-value out of mF-values is taken.

The first simulations using this protocol showed a general improvement, as well as a major variation over the different subjects. To avoid this, the data from single-channel and multichannel are combined. In particular, the best F-value out of $m + 1F$-values for each modulation frequency is taken: mF-values from multichannel calculations and one extra F-value from the original single-channel reference method.

One should be aware that this combination of both the single-channel and multichannel approach does not necessarily ensure a better performance, compared to the single-channel reference method. As it is important to keep the sensitivity of the combined processing equal to the sensitivity of the reference method, the single-channel data should truly be viewed as an extra channel, which raises the detection threshold accordingly due to the multiple testing aspect (Section III-A).

3) Single-Channel ICA: Single-channel ICA contradicts the intuition that ICA is only suitable for processing of multichannel measurements. However, if one-channel data is divided in different channels (say, two), it is considered likely the algorithm is able to extract two components with the following characteristics. The first component may be the ASSR of interest, which is presumed to be present in both (divided) channels, in the form of a sinusoid at a certain frequency. The second component may be the background EEG noise. One may argue that the nonstationary EEG noise varies too much over the two created channels. However, the chance that the statistical properties of the EEG noise from the first channel are totally different from those of the EEG noise of the second channel, is considered low.

A limitation of the ICA technique is that the number of m ICs cannot exceed the number of n observations or channels. Otherwise the ICs are not identifiable because $\mathbf{A}$ is not invertible. Therefore, no more than one IC can be estimated from single-channel data, and then - quite trivially - this IC would be equal to the original data. To avoid this problem, the available data has to be split up to create $n - 1$ extra artificial channels, so that n channels are available to calculate m ICs.

A schematic overview of the used technique is shown in Fig. 1. For the sake of simplicity, the number of channels n and ICs m is taken equal to 2. This has been observed to be the optimal number of channels and ICs for the single-channel case (Section III-D).

The single-channel procedure is as follows:

- *Step 1)* An $N \times M$ matrix is constructed from the data stream originating from the single-channel recording system described in Section II-A, with $N = 48$ the number of sweeps and $M = 4096$ the number of samples per sweep. No averaging has been carried out yet. This matrix is divided in $n = 2$ parts ("channels" or "observations"), by interleaving the odd and even sweeps, with $N/n = 24$ sweeps per part, each sweep M samples long. Part $j + 1$ contains sweeps $s_{1+j}, s_{3+j}, \ldots, s_{(N-1)+j}$ (for $j = 0, 1$).
- *Step 2)* Sweeps $s_{1+j}, s_{3+j}, \ldots, s_{(2k-1)+j}$ are averaged and stored in sweep $\overline{s}_{(N/n)j+k}$ of an averaged matrix (for $j = 0, 1; k = 1, \ldots, N/n$). The resulting averaged matrix has the same structure as the matrix from Step 1.
- *Step 3)* Independent Component Analysis is performed N/n times, each time using a group of $n = 2$ sweeps $\overline{s}_k$ and $\overline{s}_{(N/n)+k}$ from the matrix from Step 2 with $k = 1, \ldots, N/n$. Each element from this group of sweeps

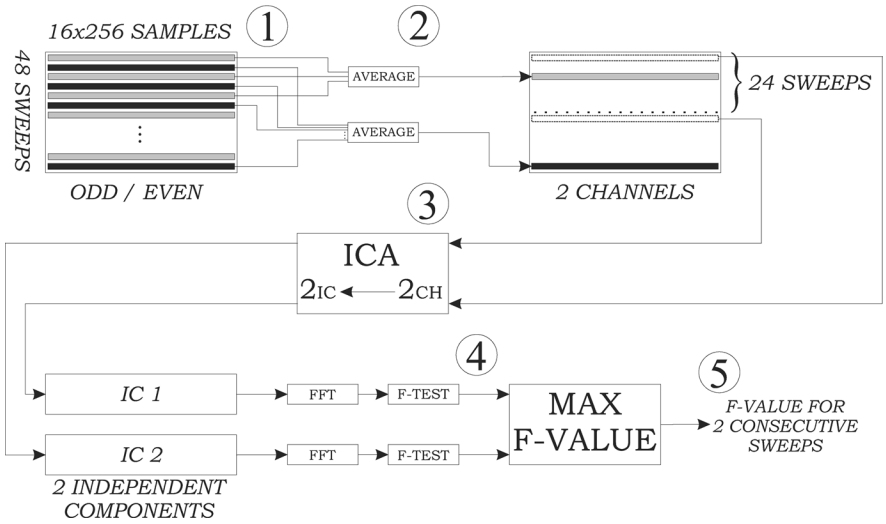

Fig. 1. Data flow for ICA applied on single-channel data. Artificial input channels are created by splitting the available data in n different parts. These n parts are used to calculate m independent components. For the sake of simplicity, n and m are taken equal to 2 for this figure.

shares the property that the element is constructed by averaging k sweeps from the matrix from Step 1. For each k, the JADE algorithm takes in $n = 2$ observations and returns $m = 2$ ICs, which are linear combinations of sweeps $\overline{s}_k$ and $\overline{s}_{(N/n)+k}$.

- *Step 4)* For each k, every IC from Step 3 is Fourier transformed and an F-test is carried out at the modulation frequency of interest. Because ICA does not order its components in any way (rows in $\mathbf{A}$ can be permuted randomly), it is unknown which component contains the highest F-value at a certain modulation frequency. For each modulation frequency, all F-values from all m ICs are calculated and the largest one is chosen.
- *Step 5)* After the best F-value is calculated, a dimension problem arises. If one F-value is calculated out of $n = 2$ source sweeps (channels) from an $N = 48$-sweep data stream, only $N/n = 24F$-values are available. To compensate this, each IC has to be copied n times to make comparison possible with the original, non-ICA, method. As such, the resulting sweep from an ICA operation on two source sweeps replaces those two sweeps by the resulting sweep and its copy.

D. Assumed Model

A seven-channel setup records linear combinations of an unknown number M of latent sources. When eight ASSRs are present one can assume eight latent sources to be ASSRs, as these sources are assumed to be independent from each other. This assumption is not correct anatomically when intensity, number of responses, carrier- and modulation frequency are varied [11]. However, when all these parameters are kept fixed, the assumption holds as each modulation frequency excites a different part of the brainstem [40]. This assumption is also supported by our own experience that ICA application on real EEG data shows that not all ASSRs are projected on one single independent component.

It is assumed in this model that each ASSR is generated by only one source. If not, the number of ASSR sources will be larger than eight. This however does not impact on the model and conclusions. Condensing this in a generative model, one obtains $\mathbf{x} = \mathbf{Bs} + \mathbf{n}$

$$\begin{bmatrix} x_1 \\ \vdots \\ x_7 \end{bmatrix} = \begin{bmatrix} b_{11} & b_{12} & \dots & b_{1M} \\ \vdots & \vdots & \ddots & \vdots \\ b_{71} & b_{72} & \dots & b_{7M} \end{bmatrix} \begin{bmatrix} s_{\mathrm{ASSR}_1} \\ s_{\mathrm{ASSR}_2} \\ \vdots \\ s_{\mathrm{ASSR}_7} \\ s_{\mathrm{ASSR}_8} \\ s_{\mathrm{noise}_1} \\ \vdots \\ s_{\mathrm{noise}_{M-8}} \end{bmatrix} + \begin{bmatrix} n_1 \\ \vdots \\ n_7 \end{bmatrix} \tag{3}$$

where s_{ASSR_i} $(i = 1, \dots, 8)$ are ASSR sources, s_{noise_j} $(j = 1, \dots, M-8)$ are muscle artefacts, eye blinks, brain processes, ..., and n_k $(k = 1, \dots, 7)$ are external noise sources like amplifier noise and, e.g., line noise picked up by the electrode cables.

When observing (3), each row k in $\mathbf{B}$ gives information about the SNR of a certain ASSR in the corresponding observation x_k. Therefore, it is possible to look for the x_k with the highest SNR for each ASSR source. After application of ICA ($\hat{\mathbf{s}} = \mathbf{Wx}$), $\mathbf{B}$ is replaced by $\hat{\mathbf{B}} = \mathbf{WB}$. The simulations from Section III are expected to show that $\hat{\mathbf{B}}$ returns a better SNR for an ASSR in certain components from $\hat{\mathbf{s}}$ than $\mathbf{B}$ for an ASSR in the observation vector $\mathbf{x}$. It is likely that the ICA technique can assess components $\hat{\mathbf{s}}$ this way that will be more useful for detection than the original observations $\mathbf{x}$, based on the assumption that ASSR sources have a platykurtic distribution, while the EEG noise sources have a more mesokurtic one (close to Gaussian).

E. Performance Measures

For evaluation of the proposed techniques, two methods have been chosen. The first one uses receiver operating characteristic (ROC) curves. It has the possibility to indicate statistically significant differences between techniques. However, ROC-curves do not give insight in the absolute benefit from one method compared to another one in terms of measurement time. Therefore,

a second measure represents the amount of time that is needed to obtain a significant response. The drawback here is that the results do not have a statistical meaning and only give an indication for what is possible for an individual subject.

1) ROC-Curve: In order to evaluate the above described techniques, ROC curves were calculated from 8 subjects [41], [42]. The curves were constructed as follows for a certain number of averaged sweeps.

1) Select 50 decision criteria p_i, represented by p-values that vary between 0.9 and 10^{-15}.
2) For each decision criterium p_i, calculate the sensitivity $\mathrm{TP}/\mathrm{TP}+\mathrm{FN}$ and specificity $\mathrm{TN}/\mathrm{FP}+\mathrm{TN}$ over all measurements (4 intensities per subject), using 16 modulation frequencies of which 8 were used as control frequencies, as in these frequencies it was assured that only noise was present. A true-negative (TN) is a correct assessment from the algorithm that a response is present in reality. A false-positive (FP) is an uncorrect assessment that no response is present, while in reality a response is there. True-positives (TP) and false-negatives (FN) are the dual cases. All TP, TN, FP, and FN are summed together over the same decision criterium p_i and used in the above equations.
3) The ROC-curve is built up plotting the *sensitivity* as a function of the *specificity*. Each p_i defines a new point of the curve.

After plotting all 50 points of the ROC-curve, the area below the curve is calculated. The area under the curve was used as a measure of detection accuracy. This procedure is carried out for each evaluated method. These calculations were carried out each time an additional sweep was collected and averaged with previous sweeps, so that the performance could also be analyzed on a time based scale.

To statistically compare different ROC-areas, a Z-test was carried out. The z-value can be calculated using [43]

$$z = \frac{A_1 - A_2}{\sqrt{\sigma_1^2 + \sigma_2^2 - 2r\sigma_1\sigma_2}}$$

with A_1 the ROC-area calculated for method 1 (the single-channel reference method) and A_2 the ROC-area calculated for method 2 (single-channel or multichannel ICA). Here, σ_i is the standard deviation of A_i and r is the correlation coefficient between the data obtained from method 1 and method 2. The σ_i are calculated using

$$\sigma_i = \sqrt{\frac{X_1 + X_2 + X_3}{n_A n_N}}$$

with

$$\begin{aligned} X_1 &= A_i(1 - A_i) \\ X_2 &= (n_A - 1)(Q_1 - A_i^2) \\ X_3 &= (n_N - 1)(Q_2 - A_i^2) \\ n_A &= \mathrm{TP} + \mathrm{FN} \\ n_N &= \mathrm{TN} + \mathrm{FP} \\ Q_1 &= \frac{A_i}{2 - A_i} \\ Q_2 &= \frac{2A_i^2}{1 + A_i} \end{aligned}$$

where n_A are all "abnormal" (positive in reality) cases and n_N all "normal" (negative in reality) cases. To find r, a value must be looked up in [43, Table I] using r_N, r_A, A_1 and A_2. Here, r_N is the Pearson Product-moment correlation between all processed normal data (n_N) from method 1 and method 2. In the same way, r_A is calculated with all abnormal data (n_A). As an alternative, r can be taken as the mean of r_A and r_N which produces a maximum error on r of 10%.

2) Effective Measurement Time Reduction: ROC-curves provide a theoretical means to assess different methods. To evaluate the practical applicability of a method, a measure for the effective benefit can be obtained by counting the number of processed sweeps until a response is first-detected. The difference between these numbers obtained with the two methods is an indication for a practical improvement or decline. In this paper, we define a first-detection to be valid when the response is significantly present for three consecutive sweeps for the single-channel and multichannel ICA method, and six consecutive sweeps for the combination of both methods. This quantity is based on the condition that there is no improvement allowed for noise frequencies when comparing ICA methods and the single-channel reference method. One needs to keep in mind this evaluation method is patient dependent and relies much on the used detection criterion.

III. Results

Figs. 2, 4, and 5–7 show the area under the ROC-curve as a function of the number of averaged sweeps for different techniques (reference method versus single-channel ICA and multichannel ICA). The reference method is the standard single-channel MASTER setup [30] with artefact rejection at 20 μV and with the amplified difference between Cz and Oz as EEG signal. A paired Z-test was carried out (Section II-E) to compare the different techniques statistically using ROC-curves. The dotted lines in Figs. 2, 6, and 7 denote two standard deviations of the ROC-areas. When they do not overlap, a significant difference is present (94.7% significance interval, two standard deviations). Important for clinical application is the fact that, with the current sampling rate of 250 Hz, a real-time calculation during measurement is possible. Every 16.384 s, a new sweep is read. On a high-end PC (Pentium 4), the calculation time of the seven-channel ICA does not exceed 5 s. As a result, each new sweep can be downsampled, processed online and visualised before the next one is collected.

A. Multichannel ICA: Seven Channels and Seven Extracted Components

1) ROC: Fig. 2 shows the results of ICA on a seven-channel input and a seven-IC output, combined with an additional channel from the single-channel reference method (Cz-Oz from Table I). A significant difference (two standard deviations) between the single-channel reference method and multichannel ICA configuration is present from sweep 11 on. The best performance of the single-channel reference method is obtained after 48 sweeps of data collection. In contrast, a significantly better performance than the single-channel reference method will ever achieve, is reached after 23 sweeps by the multichannel ICA technique. This can be interpreted as a measurement time reduction of 52%, in terms of ROC-area.

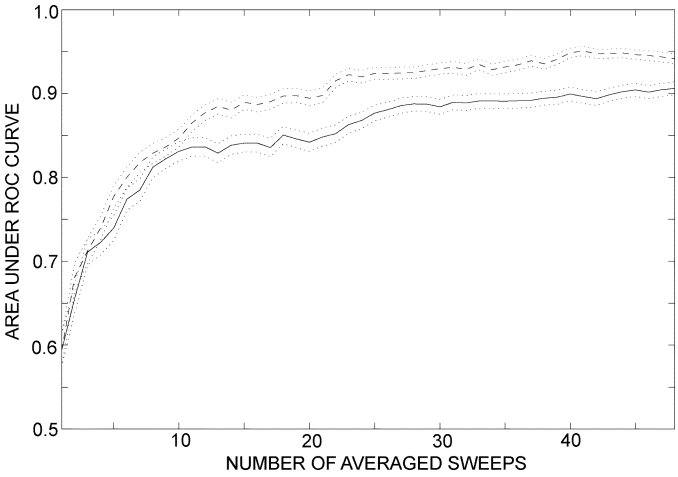

Fig. 2. Area under ROC-curve versus number of averaged sweeps: combination of $m = 7$ independent components, obtained from $n = 7$ channels, and one channel from the single-channel reference method (dashed), and single-channel reference method (solid). The dotted lines denote two standard deviations.

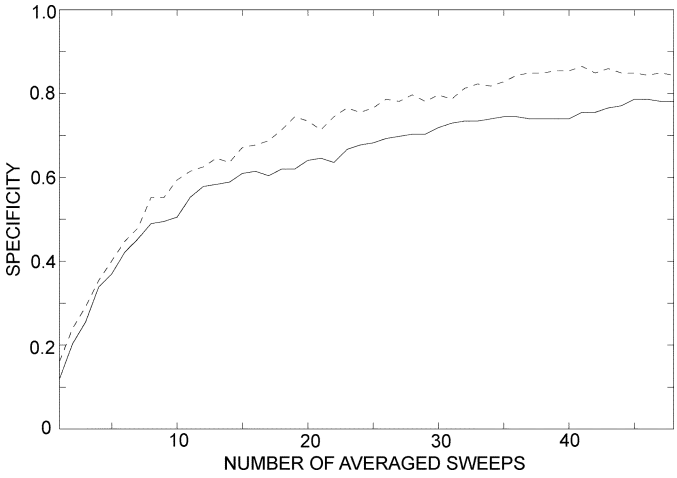

Fig. 3. Specificity versus number of averaged sweeps: combination of $m = 7$ independent components, obtained from $n = 7$ channels, and one channel from the single-channel reference method (dashed, $p = 0.0065$), and single-channel reference method (solid, $p = 0.050$). The sensitivity is taken equal to 95.0%.

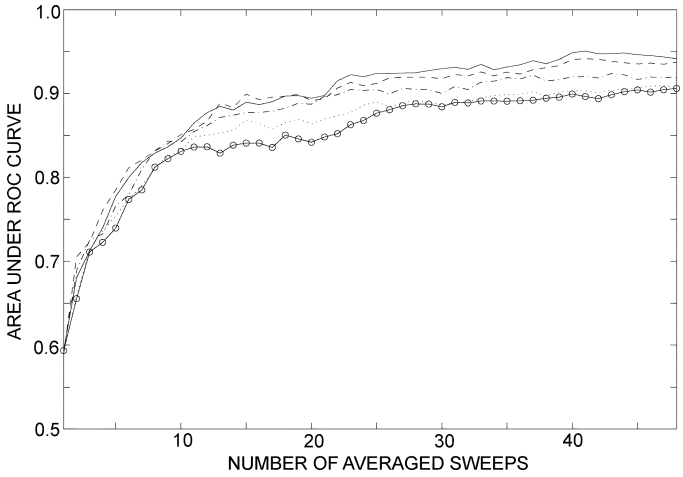

Fig. 4. Area under ROC-curve versus number of averaged sweeps. Combination of m independent components, obtained from $n = 7$ channels, and one channel from the single-channel reference method: $m = 7$ (solid), $m = 6$ (dashed), $m = 4$ (dashed-dotted), $m = 2$ (dotted), and reference method (solid-circle).

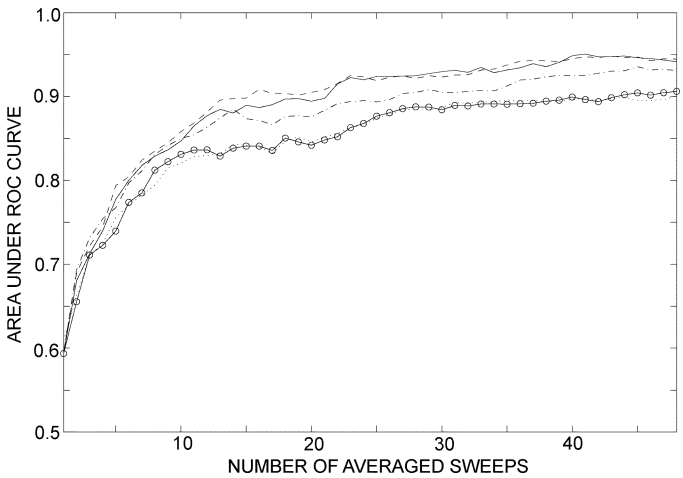

Fig. 5. Area under ROC-curve versus number of averaged sweeps. Combination of $m = n$ independent components, obtained from n channels, and one channel from the single-channel reference method: $n = 7$ (solid), $n = 5$ (dashed), $n = 4$ (dashed-dotted), $n = 2$ (dotted), and reference method (solid-circle).

It is important to know that this improvement is only caused by the use of the ICA technique, and not by the benefit of using multiple channels instead of one. If the ICA technique is omitted, for example by substituting the separating matrix $\mathbf{W}$ by the unity matrix $\mathbf{I}$, the ROC-curves will coincide.

2) Specificity and Sensitivity: Because ROC-areas are a global evaluation using an integration over a range of decision criteria (p-values), a biased representation is possible. Therefore, the sensitivity and specificity was checked for a fixed p-value that is most used in literature. Using the single-channel reference method, a p-value of 5% corresponds to a sensitivity, or TP rate, of 95%. This means that from 100 situations without a response, 5 will still be interpreted as if a response is present, due to noise influences. If more channels are evaluated simultaneously, which is the case for the ICA technique, the multiple testing aspect raises the number of FNs and, thus, lowers the sensitivity if the p-value is kept constant. To avoid this, the decision criterion for response detection is made more stringent to achieve the same sensitivity. In the case of seven-channel ICA, combined with the single-channel reference method, the effect of selecting the best out of 8 available channels forced the p-value to be lowered by a factor of 7.7 (from $p = 0.050$ to $p = 0.0065$). The reason for not applying a full Bonferroni correction [44] of a factor of 8 could be explained by the fact that there is still some dependence left between the different ICs and the additional channel. This dependence causes the full correction by a factor of 8 to be too extreme [45]. Fig. 3 shows the specificity for both methods at a sensitivity of 95.0%, which provides a more realistic view of detection performance. The detection criterion was lowered to $p = 0.0065$ for the ICA technique (with additional channel from the reference method), which still outperforms the reference method.

3) Effective Measurement Time Reduction: A comparison of both methods per subject, intensity and carrier frequency is shown in Table II. On average a mean detection time decrease

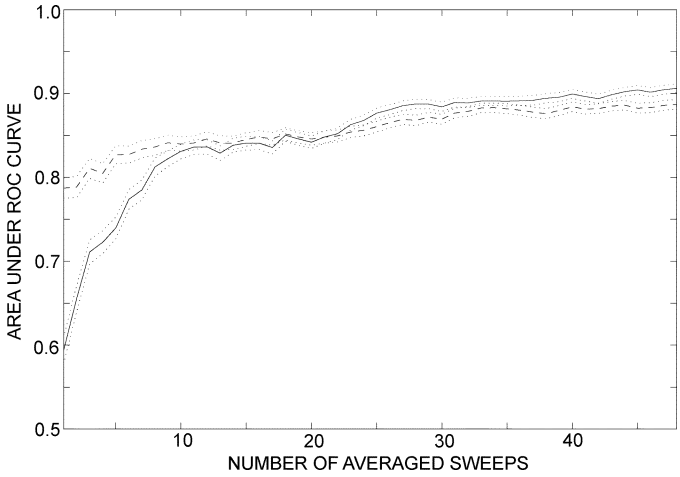

Fig. 6. Area under ROC-curve versus number of averaged sweeps: combination of splitting single-channel data into two parts (without ICA step) and one corresponding channel from the single-channel reference method (dashed), single-channel reference method (solid). The dotted lines denote two standard deviations.

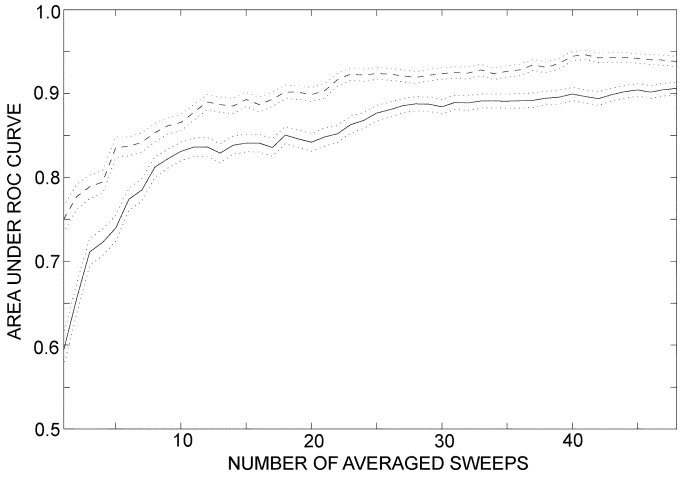

Fig. 7. Area under ROC-curve versus number of averaged sweeps: combination of $m = 7$ independent components, obtained from $n = 7$ channels, two splitted single-channel data channels and one corresponding channel from the single-channel reference method (dashed), single-channel reference method (solid). The dotted lines denote two standard deviations.

TABLE II
TIME REDUCTION (IN PERCENT) PER SUBJECT, INTENSITY AND CARRIER FREQUENCY FOR COMBINATION OF SEVEN-CHANNEL ICA AND ONE CHANNEL FROM THE SINGLE-CHANNEL REFERENCE METHOD. FIGURES RELATIVE TO THE SINGLE-CHANNEL REFERENCE METHOD. A RESPONSE IS CONSIDERED PRESENT IF IT IS SIGNIFICANT FOR 3 CONSECUTIVE SWEEPS. SIGNIFICANCE IS REACHED AT $p = 0.050$ FOR THE SINGLE-CHANNEL REFERENCE METHOD AND $p = 0.0065$ FOR THE SEVEN-CHANNEL ICA METHOD COMBINED WITH THE EXTRA SINGLE-CHANNEL. SENSITIVITY IS EQUAL TO 95.0% FOR BOTH METHODS

subject	1	2	3	4	5	6	7	8
%	8	-1	30	-2	13	8	63	19
intensity (dBSPL)	30		40		50		60	
%	25		8		22		32	
carrier (Hz)	500		1000		2000		4000	
%	15		25		31		12	

of 17% is obtained. The use of ICA yields a major decrease of the detection time for one subject (63%). For two subjects no improvement is obtained, taking into account that the standard deviation on the measurement time difference for noise frequencies is almost 5% (with a mean of 0%). This shows that these numbers vary considerably inter-subject. They can be used to indicate some underlying trends. The data concerning intensity and carrier frequency dependecies show a possible correlation between detection time reduction and SNR. Higher intensities and frequencies with physically larger responses (like 1 and 2 kHz carriers) are more prone to faster detection using ICA.

B. Multichannel ICA: Variable Number of Channels and Extracted Components

Fig. 4 shows the performance of a seven-channel system decomposed into m ICs. It is observed that performance is maximised when the number of ICs is taken as large as possible ($m = 7$) and decreases when the number of ICs goes down. The number of responses present in the data set does not influence this observation.

Fig. 5 shows the obtained results as a function of the number of channels used in the ICA method. The order of Table I was respected to construct the figure, except for the two-channel case (usage of channel 1 and channel 4, corresponding to channel 4 minus channel 1 of the single-channel reference method). An n-channel ICA, thus, used the first n channels of the table. It can be observed that a saturation effect appears after 5 channels. There is no improvement when using a multichannel recording with more than 5 channels (or 7 electrodes). After permuting through all possible combinations of 5 channels in Table I, the most optimal combination was obtained if 4 electrodes were located on the back of the head (Oz, P4, P3, Cz). According to the current dataset, the fifth electrode should be placed at F4. When other combinations were chosen, performance significantly degraded. Focussing on individual subjects in terms of effective measurement time reduction, only 2 out of 8 showed a slightly (nonsignificantly) better performance when the contralateral electrode F3 was taken instead of F4. The same result was noticed for 1 out of 4 frequencies and for 1 out of 4 intensities. This does not imply an interaction between electrode position and intensity or frequency is present.

C. Multichannel ICA: Effects of Keeping Separating Matrix Fixed

This section illustrates the effects of keeping separating matrix $\mathbf{W}$ fixed per subject or for all subjects. ICA is performed once and $\mathbf{W}$ is calculated at highest intensity (60 dBSPL) and after a complete measurement of 48 sweeps. Afterwards no ICA is applied and the same $\mathbf{W}$ is used for all further calculations of the ICs.

1) Fixed Separating Matrix for All Subjects: One fixed $\mathbf{W}$ matrix (random subject, 60 dBSPL, 48 sweeps) is used to compute the ICs of all subjects. In general, no improvement is noticed compared to the single-channel reference method. However, for the dataset used here, some $\mathbf{W}$ matrices (e.g., $\mathbf{W}$ calculated from subject 3), return a significantly better result close to the performance of standard seven-channel ICA from Section III-A. However, it is not possible to predict *a priori* an optimal $\mathbf{W}$ matrix (or a subject that provides this matrix) that maximises the performance of multichannel ICA.

TABLE III
TIME REDUCTION (IN PERCENT) PER SUBJECT, INTENSITY AND CARRIER FREQUENCY FOR COMBINATION OF SPLITTING SINGLE-CHANNEL DATA INTO TWO PARTS (WITHOUT ICA STEP) AND ONE CORRESPONDING CHANNEL FROM THE SINGLE-CHANNEL REFERENCE METHOD. FIGURES RELATIVE TO THE SINGLE-CHANNEL REFERENCE METHOD. A RESPONSE IS CONSIDERED PRESENT IF IT IS SIGNIFICANT FOR 3 CONSECUTIVE SWEEPS. SIGNIFICANCE IS REACHED AT $p = 0.050$ FOR THE SINGLE-CHANNEL REFERENCE METHOD AND $p = 0.020$ FOR THE SINGLE-CHANNEL SPLITTING METHOD COMBINED WITH THE EXTRA SINGLE-CHANNEL. SENSITIVITY IS SET AT 95.0% FOR BOTH METHODS

subject	1	2	3	4	5	6	7	8
%	-1	16	10	8	23	23	4	2
intensity (dBSPL)	30		40		50		60	
%	7		4		19		29	
carrier (Hz)	500		1000		2000		4000	
%	8		9		3		27	

TABLE IV
TIME REDUCTION (IN PERCENT) PER SUBJECT, INTENSITY AND CARRIER FREQUENCY FOR COMBINATION OF SEVEN-CHANNEL ICA, ONE CHANNEL FROM THE SINGLE-CHANNEL REFERENCE METHOD AND TWO CHANNELS OBTAINED BY SPLITTING THE AVAILABLE SINGLE-CHANNEL DATA. FIGURES RELATIVE TO THE SINGLE-CHANNEL REFERENCE METHOD. A RESPONSE IS CONSIDERED PRESENT IF IT IS SIGNIFICANT FOR 6 CONSECUTIVE SWEEPS. SIGNIFICANCE IS REACHED AT $p = 0.050$ FOR THE SINGLE-CHANNEL REFERENCE METHOD AND $p = 0.0053$ FOR THE COMBINATION METHOD. SENSITIVITY IS EQUAL TO 95.0% FOR BOTH METHODS

subject	1	2	3	4	5	6	7	8
%	13	13	30	24	18	6	58	15
intensity (dBSPL)	30		40		50		60	
%	16		15		41		45	
carrier (Hz)	500		1000		2000		4000	
%	10		33		31		25	

2) Fixed Separating Matrix for One Subject: The effect of keeping $\mathbf{W}$ fixed for each subject separately is significant for some cases. However, performance is significantly worse than the results from Section III-A.

3) Fixed IC for One Subject: By additionally fixing the component with the highest SNR for a certain modulation frequency and for the same subject (together with a fixed $\mathbf{W}$), the multiple testing aspect was avoided. The detection criterion for ICA-processed data rose from $p = 0.0065$ to $p = 0.03$ (best of fixed IC and single-channel reference method) for a sensitivity of 95.0%. However, no significant gain compared to the single-channel reference method was observed.

D. Single-Channel ICA

Following the technique described in Section II-C3, no improvement compared to the single-channel reference method was observed. However, when the single-channel ICA data was combined with one corresponding channel from the reference method, a significant benefit was visible for a lower number of averaged sweeps. Further investigation showed that the use of ICA was not even necessary here. If the separating matrix $\mathbf{W}$ is replaced by an unity matrix $\mathbf{I}$, results are almost identical. One can conclude that for a single-channel setup it is sufficient to divide the available channel in two parts and then take the best result. The ICA contribution can be removed here.

Fig. 6 displays the results for the combination of splitting single-channel data into two parts (without ICA step) and one channel from the single-channel reference method. The best results were achieved with division into two parts. A severe degradation of performance was observed when the signal was divided in more than two parts. When one of two parts originated from a different simultaneous channel, no improvement was noticed anymore (this can be verified in Fig. 5 with $m = n = 2$). The first 9 sweeps show a significant improvement. A drawback of this method is the significantly worse performance for a higher number of averaged sweeps. For a more practical approach, Table III shows a comparison of both methods per subject, intensity and carrier frequency. A measurement time reduction of almost 11% is possible.

E. Combining Single-Channel and Multichannel Techniques

1) ROC: Comparing Figs. 2 and 6, the idea of combining both methods came forward. Fig. 7 shows the ROC-curve of a method that combines single-channel and multichannel results. The benefits of both methods merge into a scheme that provides significant improvement over the whole range of averaged sweeps. In the end, the combination of both single-channel as multichannel methods can be seen as a ten-channel system: 7 multichannel ICs, 1 reference method single-channel and 2 channels obtained by splitting the available single-channel data using Section II-C3. Again, for each modulation frequency and averaged sweep, the largest SNR out of 10 calculated SNR values is taken.

2) Effective Measurement Time Reduction: By introducing two additional channels compared to the combined multichannel method, the detection criterion is reduced from $p = 0.0065$ to $p = 0.0053$, which is close to the predicted statistical value of $p = 0.005$ for a ten-channel system when taking the multiple testing aspect into account if one desires a specificity of 95.0%. These corrected decision criteria were used to construct Table IV. It confirms a further reduction of measurement time. For this dataset, the responses for all individual subjects can be detected up to 58% and on average about 22% faster. No negative values are present which however does not imply that negative values are not possible anymore. All conclusions from Section III-B, stating that the optimal number of channels is equal to five, still hold.

IV. DISCUSSION

A. Multichannel ICA: Seven Channels and Seven Extracted Components

A major improvement in detection speed is possible when recorded multichannel EEG data is preprocessed using the ICA technique prior to statistical analysis. ASSRs are sinusoidal which is characterised by a platykurtic distribution, while EEG noise sources can be considered to have mesokurtic, or Gaussian, distributions. This is in line with the central limit theorem expliciting that the combined sum of all noise sources will take on a Gaussian distribution if the number of noise sources goes to infinity [33]. As ICA is trying to separate the

sources that have optimally different distributions (statistical independence), it is probable that the algorithm is indeed able to separate the sources because of these characteristics. This separation ability is influenced by the amount of noise that is present in the used measurements. ICA performs better when less noise is present [25]. The lower the SNR, the smaller the measurement time reduction. This is reflected in Tables II and III, where especially measurements at higher intensities and with carrier frequencies that evoke larger responses (1 and 2 kHz) tend to return a larger measurement time reduction. More noise induces a worse estimation of the separating matrix $\mathbf{W}$. This is especially obvious when not using the averaging step which initially preprocesses the data solely to increase the SNR. This indicates that ICA would only be useful when applied to data with high SNR, like ASSR data at relatively high intensities above hearing threshold. Current research indicates this seems not correct however. Effects of ICA on low-intensity data at hearing threshold is subject of further research.

Two observations can be deduced from Table II: the possibility to perform worse than the single-channel reference method for some subjects and the large variance on the individual subject measurement time reduction. First, it is clearly possible that the SNR of a response can trigger a detection criterion for the single-channel case, but not the criterion for the multichannel case, which is much more stringent. This behavior can be considered as a sort of "noise floor" which could even result in a measurement time reduction for frequencies with no response present. As such, response measurement time increases which lie within the noise floor variance ($\pm 5\%$) can be neglected. Second, the large variance (data ranging from -2% to 63% and already mentioned in Section II-C2) is caused by the sometimes failing ability of the single-channel method to detect responses, even at high intensities. In practice, this can happen from time to time, and cannot be explained immediately. It is generally assumed that the Cz-Oz electrode combination is the best one for detecting responses. This assumption is not always correct and should be investigated further, as shown in [22] and [23].

B. Multichannel ICA: Variable Number of Channels and Extracted Components

Connecting many electrodes to the subject's head, is not very practical. To reduce preparation time, it is considered an advantage if a method requires fewer measurement electrodes. For this dataset, ICA applied to ASSR reaches a saturation level at 5 channels (7 electrodes). This could indicate that it is sufficient to condense all estimated sources $\hat{\mathbf{s}}$ from Section II-D in only five major components $\hat{s}_i$, each component being a combination of several ASSRs and noise sources. If more channels are used, no performance improvement is observed anymore. This effect can be explained by the fact that a sixth channel still adds extra information to the complete system, but this additional gain is annihilated by the extra increase of FNs (detections) caused by the addition of an extra channel. This explanation is valid for both multichannel ICA as the combination of single-channel and multichannel methods from Section IV-E. The best electrode positions are located on the back of the head. This was expected because of the higher SNR that is obtained at these positions [22]. For this dataset, the additional fifth channel should be located in between the four channels on the back of the head and the forehead, more specifically on position F4. The choice for the symmetrical electrode position F3 degenerates the performance. This is due to some inter-subject variability.

C. Multichannel ICA: Effects of Keeping Separating Matrix Fixed

1) Variability of the Separating Matrix: The reconstruction of the assumed underlying generators $\hat{\mathbf{s}}$ from Section II-D is performed by multiplying the computed separating matrix $\mathbf{W}$ with the signal matrix $\mathbf{x}$. As a result, the obtained ICs are an optimal linear combination of the recorded signals in a non-Gaussian and independent sense. The elements of matrix $\mathbf{W}$ are determined by several factors, like the position and quality of the electrodes, the location and orientation of the underlying sources inside, and the physical properties of the subject's skull. During one subject session with different intensities, these parameters are sufficiently stationary. This is reflected in reoccuring ICs with similar structure (combinations of different responses) for the same intensity and even for different intensities, as long as one and the same subject is considered. Almost the same holds for the separating matrices $\mathbf{W}$. When comparing two $\mathbf{W}$ matrices that originate from different datasets, but close to each other on a time scale, the matrix coefficients differ only slightly with sometimes permuted rows. The similarities of these matrices are caused by the high correlation between an averaged sweep and its successor. This behavior is not observed when comparing $\mathbf{W}$ matrices from the same subject but at different intensities.

2) Fixed Separating Matrix for All Subjects: Keeping $\mathbf{W}$ fixed for all subjects yields good performance as long as the correct $\mathbf{W}$ is chosen. However, the major problem is the choice of $\mathbf{W}$. For some separating matrices, a performance close to that of the standard use of ICA is reached. This could indicate that an optimal separating matrix can be calculated *a priori* for a multichannel setup. However, this matrix can only be used for a certain electrode configuration and data set, if it already can be found in the first place. If so, the calculation for each new averaged sweep of the $\mathbf{W}$ coefficients will likely perform better.

3) Fixed Separating Matrix for One Subject: The ROC-curves show that fixing $\mathbf{W}$ calculated from data with the largest assumed SNR from each subject, can reduce detection time significantly. However, this improvement is still significantly smaller than the improvement obtained when ICA is applied every time to each collected, averaged, sweep. The former results show that the derived ICs represent corresponding real physical entities that change between subjects and intensities, but stay rather constant for the same intensity.

4) Fixed IC for One Subject: Fixing ICs per modulation frequency should be avoided. Although it seems interesting without the multiple testing aspect (and, therefore, a less stringent detection criterion needs to be used), it is not advisable to link a component to a modulation frequency immediately. ICA does not order its ICs. Therefore, a fixed IC can not be chosen beforehand. One can try to solve this problem by introducing an ordering system, like sorting ICs according to their energy. This however, will not always work, especially at lower SNRs. This observation can be explained by model (3). Depending on the variable composition of $\mathbf{s}$, fixed components or fixed $\mathbf{W}$

will give variable results, without the existance of an optimal solution.

D. Single-Channel ICA

In general, ICA does not work on single-channel data. This is expected because ICA is essentially a multichannel technique. When multiple channels are recorded simultaneously, ICA uses the relatively high correlation between the different channels to separate mesokurtic background noise and leptokurtic responses. When only one channel is available, the different parts apparently do almost not have any correlation at all because EEG signals are too nonstationary. Our assumption does not seem to be valid.

E. Combining Single-Channel and Multichannel Techniques

The better performance at lower SNRs when splitting the single-channel data cannot be explained yet. A careful first guess could be that one should avoid to work with entire groups of samples (and, thus, probability distributions, like ICA), but should try to combine data sample-by-sample-wise. The creation of two extra channels seems to return a higher benefit than the drawback it creates by lowering the detection threshold. This, however, is only valid when the two extra channels are created from one and the same channel. This indicates this method makes use of similar noise characteristics throughout the same channel.

F. Multichannel ICA: The Use of Artefact Rejection

In this paper, artefact rejection was used to define the reference approach as close as possible to the clinically standard single-channel technique. All epochs that contain samples with a value higher than 20 μV in absolute value, were rejected. In theory, ICA can separate external sources (muscles, eye blinks, etc.) easily from the actual EEG that is being monitored. In practice, the benefits of ICA have already been confirmed when noisy subject data are considered, as long enough channels are used [46]. The single-channel reference method however is incapable of extracting any useful information from data contaminated with much noise and artefacts, which is indeed experienced, e.g., by clinical people who have to test restless babies. When multichannel recordings are used, we observed that even the noisiest input data to some extent still can be processed to usable ASSRs, even with a relatively small number of available channels. This is subject of further research.

V. Conclusion

In this paper, it is shown that ICA is a valuable tool to separate the additive background noise from the EEG-waveform of interest, namely the ASSR. ICA applied on single-channel and multichannel recordings yields a significantly better performance than the clinically used single-channel reference technique for data obtained at intensities above hearing threshold. For single-channel measurements a time reduction up to 23% for a single subject has been acquired. For multichannel EEG measurements there is a significant measurement time reduction possible of 52% for 48-sweep measurements compared to the single-channel reference technique. For individual subjects, an improvement up to 63% in measurement time has been recorded. When both single-channel and multichannel techniques are combined, performance can be improved even more. This ultimate combination generally guarantees a significant improvement for all measurement durations. However, multichannel ICA is not always capable of reducing measurement time for each individual subject, illustrating inter-subject variability of ICA-ASSR and/or ASSR in general.

Five-channel ICA yields the same performance as the seven-channel ICA. This is important for the clinical applicability of the described technique. When the separating matrix $\mathbf{W}$ is kept fixed for each subject seperately, a significant improvement is observed for some cases. Keeping $\mathbf{W}$ fixed for all subjects improves detection speed significantly, as long as an optimal $\mathbf{W}$ is found *a priori*. This, however, is not always garantueed.

References

[1] Joint Committee on Infant Hearing, "1994 position statement," *Pediatrics*, vol. 95, no. 1, pp. 152–156, 1995.

[2] H. Luts and J. Wouters, "Hearing assessment by recording multiple auditory steady-state responses: The influence of test duration," *Int. J. Audiol.*, vol. 43, no. 8, pp. 471–478, 2004.

[3] H. Luts, C. Desloovere, and J. Wouters, "Clinical application of dichotic multiple-stimulus auditory steady-state responses in high-risk newborns and young children," *Audiol. Neuro-Otol.*, vol. 11, pp. 24–37, 2006.

[4] D. Regan, *Human Brain Electrophysiology: Evoked Potentials and Evoked Magnetic Fields in Science and Medicine*. Amsterdam, The Netherlands: Elsevier, 1989.

[5] M. Aoyagi, T. Kiren, Y. Kim, Y. Suzuki, T. Fuse, and Y. Koike, "Optimal modulation frequency for amplitude-modulation following response in young children during sleep," *Hear. Res.*, vol. 65, pp. 253–261, 1993.

[6] M. Aoyagi, T. Kiren, H. Furuse, T. Fuse, Y. Suzuki, and M. Yokoto, "Pure-tone threshold prediction by 80-Hz amplitude-modulation following response," *Acta Otolaryngol.*, vol. suppl 511, pp. 7–14, 1994.

[7] L. T. Cohen, F. W. Rickards, and G. M. Clark, "A comparison of steady state evoked potentials to modulated tones in awake and sleeping humans," *J. Acoust. Soc. Am.*, vol. 90, pp. 2467–2479, 1991.

[8] G. Rance, F. W. Rickards, L. T. Cohen, S. De Vidi, and G. M. Clark, "The automated prediction of hearing thresholds in sleeping subjects using auditory steady-state evoked potentials," *Ear Hear.*, vol. 16, pp. 499–507, 1995.

[9] F. W. Rickards, L. E. Tan, L. T. Cohen, O. J. Wilson, J. H. Drew, and G. M. Clark, "Auditory steady state evoked potentials in newborns," *Br. J. Audiol.*, vol. 28, no. 6, pp. 327–337, 1994.

[10] O. G. Lins, P. E. Picton, T. W. Picton, S. C. Champagne, and A. Durieux-Smith, "Auditory steady-state responses to tones amplitude-modulated at 80-110 Hz," *J. Acoust. Soc. Am.*, vol. 97, pp. 3051–3063, 1995.

[11] O. G. Lins and T. W. Picton, "Auditory steady-state responses to multiple simultaneous stimuli," *Electroencephalogr. Clin. Neurophysiol.*, vol. 96, pp. 420–432, 1995.

[12] M. S. John, A. Dimitrijevic, P. Van Roon, and T. W. Picton, "Multiple auditory steady-state responses (MASTER): Stimulus and recording parameters," *Audiology*, vol. 37, pp. 59–82, 1998.

[13] M. S. John, D. W. Purcell, A. Dimitrijevic, and T. W. Picton, "Advantages and caveats when recording steady-state responses to multiple simultaneous stimuli," *J. Acoust. Soc. Am.*, vol. 13, pp. 246–259, 2002.

[14] R. A. Dobie and M. J. Wilson, "A comparison of t test, f test, and coherence methods of detecting steady-state auditory-evoked potentials, distortion-product otoacoustic emissions, or other sinusoids," *J. Acoust. Soc. Am.*, vol. 100, no. 4, pt. 1, pp. 2236–2246, 1996.

[15] J. L. Valdes, M. C. Perez-Abalo, V. Martin, G. Savio, C. Sierra, E. Rodriguez, and O. Lins, "Comparison of statistical indicators for the automatic detection of 80 Hz auditory steady state responses," *Ear Hear.*, vol. 18, pp. 420–429, 1997.

[16] T. W. Picton, A. Dimitrijevic, M. S. John, and P. Van Roon, "The use of phase in the detection of auditory steady-state responses," *Clin. Neurophysiol.*, vol. 112, pp. 1698–1711, 2001.

[17] M. S. John, A. Dimitrijevic, and T. W. Picton, "Weighted averaging of steady state responses," *Clin. Neurophysiol.*, vol. 122, pp. 555–562, 2001.

[18] M. S. John, A. Dimitrijevic, and T. W. Picton, "Auditory steady-state responses to exponential modulation envelopes," *Ear Hear.*, vol. 23, pp. 106–117, 2002.
[19] M. S. John, D. K. Brown, P. J. Muir, and T. W. Picton, "Recording auditory steady-state responses in young infants," *Ear Hear.*, vol. 25, no. 6, pp. 539–553, 2004.
[20] E. Stürzebecher, M. Cebulla, and U. Pschirrer, "Efficient stimuli for recording of the amplitude modulation following response," *Audiology*, vol. 40, pp. 63–68, 2001.
[21] R. Mühler, F. von Dobeneck, M. Ziese, and H. von Specht, "Recording of multiple frequency ASSR with adaptive stimuli," in *The 19th International Evoked Response Audiometry Study Group (IERASG) Biennial Symposium*, Havana, Cuba, 2005.
[22] C. S. van der Reijden, L. H. M. Mens, and A. F. M. Snik, "EEG derivations providing auditory steady-state responses with high signal-to-noise ratios in infants," *Ear Hear.*, vol. 26, pp. 299–309, 2005.
[23] C. S. van der Reijden, L. H. M. Mens, and A. F. M. Snik, "Signal-to-noise ratios of the auditory steady-state response from fifty-five EEG derivations in adults," *J. Am. Ac. Audiol.*, vol. 15, no. 10, pp. 692–701, 2004.
[24] Y. Tang and A. M. Norcia, "An adaptive filter for steady-state evoked responses," *Electroencephalogr. Clin. Neurophysiol.*, vol. 96, pp. 268–277, 1995.
[25] A. Hyvärinen, J. Karhunen, and E. Oja, *Independent Component Analysis*. New York: Wiley, 2001.
[26] S. Bounkong, B. Toch, D. Saad, and D. Lowe, "ICA for watermarking digital images," *J. Mach. Learn. Res.*, vol. 4, pp. 1471–1498, 2003.
[27] H. Fang and H. De-Shuang, "Extracting mode components in laser intensity distribution by independent component analysis," *Appl. Opt.*, vol. 44, no. 18, pp. 3646–3653, 2005.
[28] L. De Lathauwer, B. De Moor, and J. Vandewalle, "Fetal electrocardiogram extraction by blind source subspace separation," *IEEE Trans. Biomed. Eng.*, vol. 47, no. 5, pp. 567–572, May 2000.
[29] A. D. Back and A. S. Weigend, "A first application of independent component analysis to extracting structure from stock returns," *Int. J. Neural Syst.*, vol. 8, no. 5, pp. 473–484, 1997.
[30] M. S. John and T. W. Picton, "MASTER: A Windows program for recording multiple auditory steady-state responses," *Comput. Meth. Programs Biomed.*, vol. 61, pp. 125–150, 2000.
[31] J. Malmivuo and R. Plonsey, *Bioelectromagnetism: Principles and Applications of Bioelectric and Biomagnetic Fields*. New York: Oxford Univ. Press, 1995.
[32] P. Comon, "Independent component analysis, a new concept?," *Signal Process.*, vol. 36, pp. 287–314, 1994.
[33] H. F. Trotter, "An elementary proof of the central limit theorem," *Arch. Math.*, vol. 10, pp. 226–234, 1959.
[34] J. Cardoso and A. Soloumiac, "Blind beamforming for non-Gaussian signals," *Inst. Electr. Eng. Proc.-F*, vol. 140, no. 6, pp. 362–370, 1993.
[35] A. Hyvärinen, "Fast and robust fixed-point algorithms for independent component analysis," *IEEE Trans. Neural Netw.*, vol. 10, no. 3, pp. 626–634, May 1999.
[36] H. Stögbauer, A. Kraskov, S. A. Astakhov, and P. Grassberger, "Least-dependent-component analysis based on mutual information," *Phys. Rev. E*, vol. 70, pp. 066 123/1–066 123/17, 2004.
[37] K. H. Knuth, "A Bayesian approach to source separation," in *Proc. ICA '99*, Aussois, France, 1999, pp. 283–288.
[38] P. Comon, "Blind identification and source separation in 2×3 underdetermined mixtures," *IEEE Trans. Signal Process*, vol. 52, no. 1, pp. 11–22, Jan. 2004.
[39] Y. Deville, M. Benali, and F. Abrard, "Differential source separation for underdetermined instantaneous or convolutive mixtures: Concept and algorithms," *Signal Process.*, vol. 84, pp. 1759–1776, 2004.
[40] T. W. Picton, M. S. John, A. Dimitrijevic, and D. Purcell, "Human auditory steady-state responses," *Int. J. Audiol.*, vol. 42, no. 4, pp. 177–219, 2003.
[41] J. A. Hanley and B. J. McNeil, "The meaning and use of the area under the receiver operating characteristic (ROC) curve," *Radiology*, vol. 143, pp. 29–36, 1982.
[42] D. Green and J. A. Swets, *Signal Detection Theory and Psychophysics*. New York: Wiley, 1966.
[43] J. A. Hanley and B. J. McNeil, "A method of comparing the areas under receiver operating characteristic curves derived from the same cases," *Radiology*, vol. 148, pp. 839–843, 1983.
[44] J. M. Bland and D. G. Altman, "Multiple significant tests: The Bonferroni method," *Br. Med. J.*, vol. 310, p. 170, 1995.
[45] E. Stürzebecher, M. Cebulla, and C. Elberling, "Automated auditory response detection: Statistical problems with repeated testing," *Int. J. Audiol.*, vol. 44, pp. 110–117, 2005.
[46] T.-P. Jung, S. Makeig, C. Humphries, T.-W. Lee, M. J. McKeown, V. Iragui, and T. J. Sejnowski, *Removing Electroencephalographic Artifacts by Blind Source Separation*. Cambridge, U.K.: Cambridge Univ. Press, , vol. 37, pp. 163–178, 2000.



Bram Van Dun (S'07) was born in 1979 in Zoersel, Belgium. He received the M.Sc. degree in electrical engineering from the Katholieke Universiteit Leuven (K.U.Leuven), Leuven, Belgium, in 2003. He is currently working toward the Ph.D. degree in engineering at the Electrical Engineering Department and at the Experimental ORL, Neurosciences Department, both at the K.U.Leuven. His research interests include biomedical signal processing in general, and EEG signal processing applied to hearing tests in particular.



Jan Wouters was born in Leuven, Belgium, in 1960. He received the physics degree and the Ph.D. degree in sciences/physics from the Katholieke Universiteit Leuven (K.U.Leuven), Leuven, Belgium, in 1982 and 1989, respectively.

From 1989-1992, he was a Research Fellow with the Belgian National Fund for Scientific Research (NFWO) at the Institute of Nuclear Physics (UCL Louvain-la-Neuve and K.U.Leuven) and at NASA Goddard Space Flight Center (Maryland). Since 1993, he is a Professor with the Neurosciences Department at K.U.Leuven. His research activities are about audiology and the auditory system, signal processing for cochlear implants and hearing aids. He has authored about 100 articles in international peer-review journals and is a reviewer for several international journals.

Dr. Wouters received an Award of the Flemish Ministery in 1989, a Fullbright Award, and a NATO Research Fellowship in 1992, and the Flemish VVL Speech therapy-Audiology Award in 1996. He is member of the International Collegium for Rehabilitative Audiology and of the International Collegium for ORL, a Board Member of the NAG (Dutch Acoustical Society).



Marc Moonen (M'94–SM'06) received the electrical engineering degree and the Ph.D. degree in applied sciences from Katholieke Universiteit Leuven (K.U.Leuven), Leuven, Belgium, in 1986 and 1990 respectively.

Since 2004, he is a Full Professor with the Electrical Engineering Department, K.U.Leuven.

Dr. Moonen received the 1994 K.U.Leuven Research Council Award, the 1997 Alcatel Bell (Belgium) Award (with P. Vandaele), the 2004 Alcatel Bell (Belgium) Award (with R. Cendrillon), and was a 1997 "Laureate of the Belgium Royal Academy of Science." He received a journal best paper award from the IEEE TRANSACTIONS ON SIGNAL PROCESSING (with G. Leus) and from *Signal Processing* (with S. Doclo). He was chairman of the IEEE Benelux Signal Processing Chapter (1998-2002), and is currently a EURASIP AdCom Member (European Association for Signal, Speech and Image Processing, 2000-), and a member of the IEEE Signal Processing Society Technicial Committee on Signal Processing for Communications. He has served as Editor-in-Chief for the *EURASIP Journal on Applied Signal Processing* (2003-2005), and has been a member of the editorial board of IEEE TRANSACTIONS ON CIRCUITS AND SYSTEMS II (2002-2003) and *IEEE Signal Processing Magazine* (2003-2005). He is currently, and a member of the editorial board of *Integration, the VLSI Journal*, *EURASIP Journal on Applied Signal Processing*, *EURASIP Journal on Wireless Communications and Networking*, and *Signal Processing*.